



Differential representations of spatial location by aperiodic and alpha oscillatory activity in working memory

Andrew Bender^{a,1}, Chong Zhao^b, Edward Vogel^{b,c}, Edward Awh^{b,c}, and Bradley Voytek^{a,d,e,f}

Affiliations are included on p. 8.

Edited by Marlene Behrmann, University of Pittsburgh, Pittsburgh, PA; received March 24, 2025; accepted June 26, 2025

Decades of research have shown working memory (WM) relies on sustained prefrontal cortical activity and visual extrastriate activity, particularly in the alpha (8 to 12 Hz) frequency range. This alpha activity tracks the spatial location of WM items, even when spatial position is task-irrelevant and no stimulus is currently being presented. Traditional analyses of putative oscillations using bandpass filters, however, conflate oscillations with nonoscillatory aperiodic activity. Here, we reanalyzed seven human electroencephalography visual WM datasets to test the hypothesis that aperiodic activity, which is thought to reflect the relative contributions of excitatory and inhibitory drive-plays a distinct role in visual WM from true alpha oscillations. To do this, we developed a time-resolved spectral parameterization approach to disentangle oscillations from aperiodic activity during WM encoding and maintenance. Across all seven tasks, totaling 112 participants, we captured the representation of spatial location from total alpha power using inverted encoding models (IEMs), replicating traditional analyses. We then trained separate IEMs to estimate the strength of spatial location representation from aperiodic-adjusted alpha (reflecting just the oscillatory component) and aperiodic activity and find that IEM performance improves for aperiodic-adjusted alpha compared to total alpha power that blends the two signals. We also identify a distinct role for aperiodic activity, where IEM performance trained on aperiodic activity is highest during stimulus presentation, but not during the WM maintenance period. Our results emphasize the importance of controlling for aperiodic activity when studying neural oscillations while uncovering a functional role for aperiodic activity in encoding visual WM information.

alpha oscillations | working memory | aperiodic activity

Working memory (WM) refers to our ability to hold and manipulate information in mind for a short time, usually just a few seconds. Although WM is core to many cognitive functions and is disrupted in numerous psychiatric and neurological disorders, the underlying neurocomputational principles of WM remain elusive. While sustained single-neuron activity in the prefrontal cortex (PFC) is considered a hallmark of WM, it relies on population coding distributed across many regions (1). Population neural activity in the PFC represents a broad array of task variables such as stimulus-stimulus association (2) and sustained representations of WM content in the pattern of activity of voxels distributed within parietal and sensory cortices (3-7).

Another way of assessing population codes is via extracellular field recordings that measure synaptic and transmembrane currents in a neural population (8). Oscillations are a common feature of these signals, and play key roles in neural communication and computation (9). Changes in oscillatory power have been documented in the delay period of WM tasks at multiple scales: from invasive local field potentials (LFPs) to noninvasive electroencephalography (EEG) and magnetoencephalography (MEG). Visual cortical alpha (8 to 12 Hz) oscillations have been implicated in WM, with both alpha power increases (10-12) and decreases (11, 13-15) during WM tasks. These seemingly paradoxical results have been resolved by differential alpha dynamics, with increased alpha power reflecting disengagement of task-irrelevant sensory representations, and decreased alpha power reflecting engagement of task-relevant sensory representations (11, 16, 17). Like its role in spatial attention, alpha power is reduced contralateral to locations held in spatial WM (18-20), with both healthy aging and unilateral PFC lesions altering visual cortical delay period alpha (21, 22). Alpha band activity also encodes the precise spatial location of WM stimuli (23, 24), even when spatial location is task-irrelevant (25).

While there is substantial evidence for changes in narrowband alpha power in visual attention and WM, oscillations occur in conjunction with nonoscillatory aperiodic

Significance

Working memory is a crucial component of cognition, yet its neural mechanisms are not fully understood. Research shows that alpha activity—presumed to reflect neural oscillations—tracks the location of items we hold in memory. However, these analyses assume that all alpha power is oscillatory, even though oscillations are mixed with nonoscillatory, aperiodic activity that may be physiologically and functionally distinct. Here, we use an analytical approach for separating alpha oscillations and aperiodic activity dynamically across time. Our results reveal distinct roles for each in human visual working memory: Aperiodic activity reflects encoding of spatial location, whereas alpha oscillations are involved in its maintenance.

Author contributions: A.B., E.V., E.A., and B.V. designed research; A.B., C.Z., E.V., E.A., and B.V. performed research; A.B. and B.V. contributed new reagents/analytic tools; A.B. analyzed data; and A.B. and B.V. wrote the

The authors declare no competing interest.

This article is a PNAS Direct Submission

Copyright © 2025 the Author(s). Published by PNAS. This open access article is distributed under Creative Commons Attribution-NonCommercial-NoDerivatives License 4.0 (CC BY-NC-ND).

¹To whom correspondence may be addressed. Email: abender@ucsd.edu.

This article contains supporting information online at https://www.pnas.org/lookup/suppl/doi:10.1073/pnas. 2506418122/-/DCSupplemental.

Published July 24, 2025.

activity. Aperiodic activity has historically been dismissed as neural noise, though given the physiological nature of the LFP (and thus, by extension, EEG), more recent work has shown that aperiodic activity likely reflects asynchronous cortical drive that is coarsely related to the relative excitatory/inhibitory drive (26, 27), and is dynamically related to cognitive and behavioral state (28-30). Critically, changes in aperiodic activity are distinct from event-related potentials (31), suggesting that event-related fluctuations in aperiodic activity are not merely a byproduct of phase-locked responses but instead reflect broadband shifts in neural excitability. Using traditional spectral analyses, such as narrowband filtering in a predefined alpha band, dynamic and task-related changes in this aperiodic activity can appear to be changes in oscillatory activity, even if no oscillation is present (32, 33). This raises the question as to whether the preponderance of evidence of alpha dynamics during WM reflects true alpha oscillations, or is actually capturing rapid fluctuations in aperiodic dynamics that manifest as power changes in the alpha frequency range, or reflects dynamic changes in both.

Here, we reanalyze seven previously published EEG experiments, totaling 112 participants, that have previously demonstrated alpha band encoding of visual WM information during a WM delay period under various task conditions. By using a timeresolved extension of spectral parameterization, we dissociate the effects of event-related alpha oscillations from aperiodic dynamics in the encoding and maintenance of WM information with subsecond resolution. Even when controlling for aperiodic dynamics, we find that alpha power represents the correct spatial location of visual items sustained across the WM delay period across all seven tasks. Importantly, this representation actually improves after controlling for aperiodic activity. This reinforces the idea that alpha oscillations—not just alpha power—represent spatial location in visual WM. We also identify a distinct role of aperiodic activity in the transient encoding of spatial information across all seven tasks, that, unlike alpha oscillations, does not sustain during the delay period but is only evident after stimulus presentation. These results highlight the importance of considering aperiodic activity in our analyses. They strengthen the evidence for the role of alpha oscillations in visual WM while hinting at a distinct role of aperiodic activity, potentially for the encoding of visual information.

Materials and Methods

Participants. The EEG data analyzed in this paper were collected from participants at the University of Oregon (n=56) and the University of Chicago (n=56). These data are from three publicly available datasets (25, 34), and the published reports contain the complete details on participants, data collection procedures, experimental design, and data preprocessing. But we summarize them briefly, here.

Experimental Design. The three publicly available datasets (24, 25, 34) encompass data from seven different tasks/experiments (Table 1), during all of which participants attended to and remembered positions of memory items around fixation, across a delay period. As shown in Fig. 1, the tasks proceeded in three stages: stimulus, delay, and response. During stimulus presentation, participants were presented with one or two simple stimuli (circles, squares, gratings, or triangles) equidistant from fixation (4° visual angle). Stimuli were presented for durations ranging from 100 ms to 1,000 ms. Following stimulus offset, there was a fixed, blank delay period containing only a fixation point where durations ranged from 1,000 to 1,750 ms depending on the dataset. Finally, during the response period, participants were presented with a response screen that contained either a ring presented around fixation (continuous recall tasks) or a single probe stimulus (change detection task). All of the tasks were continuous recall tasks except for Task 3, which was a change detection task in which the participants had 250 ms to determine whether the probe stimulus had changed from stimulus presentation.

Importantly, all tasks required that participants attend to locations around fixation either explicitly or implicitly, regardless of the response required. In the University of Oregon sample, participants were instructed to remember the spatial position (Tasks 1 to 3, n=44) or color (Task 4, n=12) of a circle stimulus presented around fixation throughout the blank delay period. In the University of Chicago sample, participants were presented with two stimuli (a square and a triangle in Task 5, two colored gratings in Task 6, and two colored circles in Task 7) and cued in advance to attend and remember only one of the stimuli based on its shape (Task 5) or color (Tasks 6 and 7). In Task 7, some of the trials featured only one colored circle and no distractor. After a brief delay, participants were required to report the color (Task 5), orientation (Task 6), or spatial position (Task 7) of the cued stimulus. Notably, all tasks required that participants attend spatial positions around fixation and encouraged participants to maintain those spatial representations through a blank delay.

EEG Recordings. EEG recordings done at the University of Oregon (Tasks 1 to 4) recorded activity from 20 electrodes, namely International 10/20 sites F3, FZ, F4, T3, C3, CZ, C4, T4, P3, PZ, P4, T5, T6, O1, and O2, along with five nonstandard sites: OL midway between T5 and O1, OR midway between T6 and O2, PO3 midway between P3 and OL, PO4 midway between P4 and OR, and POz midway between PO3 and PO4. EEG recordings done at the University of Chicago (Tasks 5 to 7) recorded activity from 26 common electrodes, namely O2, Oz, O1, P8, P4, Pz, P3, P7, CP6, CP2, CP1, CP5, T8, C4, Cz, C3, T7, FT10, FC6, FC2, FC1, FC5, FT9, F8, F4, Fz, F3, F7, FP2, and FP1. For Tasks 5 and 6, EEG activity was also recorded at PO7, PO4, PO3, and PO8, while EEG activity was recorded at T7 and T8 for Task 7. Data from all seven tasks were rereferenced offline to the algebraic average of the left and right mastoids and bandpass-filtered from 0.01 to 80 Hz. University of Oregon data was digitized at 250 Hz using LabVIEW 6.1, while University of Chicago data was digitized at 500 Hz using BrainVision Recorder (Brain Products, Munich, Germany). Finally, trials from all seven tasks were visually inspected for artifacts using EEG, EOG, and eye tracking data, such that trials were discarded if they were contaminated by blocking, blinks, detectable eye movements, excessive muscle noise, or skin potentials.

Spectral Decomposition and Time-Resolved Parameterization. Repeating the procedure from the original papers (24, 25, 34), alpha total power was computed for each trial using a narrowband alpha filter and Hilbert transform

Table 1. Task parameters across seven WM tasks and two research sites

Task	Stimulus (ms)	Delay (ms)	Response (ms)	Task-relevant feature	Type	Site	n	Dataset
1	250	1,750	Until response	Location	Recall	Oregon	15	(24)
2	1,000	1,000	Until response	Location	Recall	Oregon	15	(24)
3	250	1,750	250	Location	Change detection	Oregon	14	(24)
4	100	1,200	Until response	Color	Recall	Oregon	12	(25)
5	100	1,150	Until response	Color	Recall	Chicago	18	(25)
6	100	1,150	Until response	Orientation	Recall	Chicago	14	(25)
7	250	1,000	Until response	Location	Recall	Chicago	24	(34)

Stimulus presentation and delay timings, response type, recording site, and which feature was relevant for the WM task were variable across the tasks.

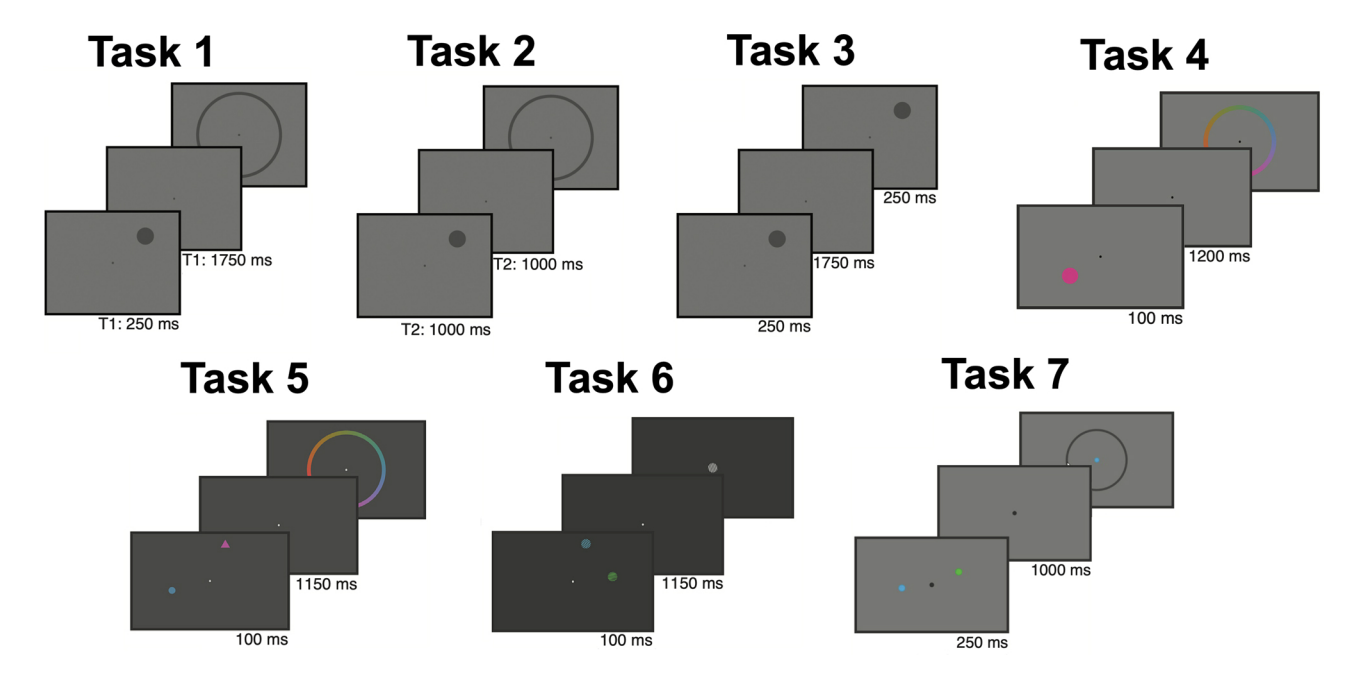


Fig. 1. Example task for each WM task. In each task, a stimulus was presented (*Front*), the participant was asked to remember a feature of the stimulus across a WM delay (*Middle*), and then reported the remembered feature value during a response period (*Bαck*).

approach. The data were filtered in the alpha band (8 to 12 Hz), and then the Hilbert transform was applied on the filtered data to get the analytic signal. The instantaneous alpha power was the magnitude of this analytic signal. This measure of instantaneous alpha power does not account for confounding contributions of aperiodic activity, and, as such, is hereafter referred to as total alpha power to disambiguate it from our subsequent analyses that separate putative oscillations from aperiodic activity.

To estimate an aperiodic-adjusted instantaneous measure of alpha power, we first computed sliding-window power spectra for each trial using multitapers in MNE-Python (35) with time windows of 1 s (Fig. 2B). This procedure resulted in power estimates for 128 frequencies, from 2 to 50 Hz, from which the "instantaneous" spectral parameters could be estimated. It is important to emphasize that "instantaneous" analytics amplitude using the traditional filter-Hilbert approach has similar temporal uncertainty as our sliding-window shorttime Fourier-multitaper approach (36). Spectral decomposition of these timefrequency representations was then done using the spectral parameterization method (version 1.1.0) (Fig. 2C) (32). Settings for the algorithm were set as follows: peak width limits: (2, 8); max number of peaks: 4; minimum peak height: 0; peak threshold: 2.0; and aperiodic mode: "fixed." Power spectra were parameterized across the frequency range 2 to 50 Hz. We extracted the aperiodic exponent from these model fits, providing an estimate of the "instantaneous" aperiodic exponent for each time point in each trial (Fig. 2D, orange line). Finally, we estimated the instantaneous aperiodic-adjusted alpha power by subtracting the aperiodic activity from the power spectra for each time point and calculated the area under the curve (AUC) on a linear scale in the alpha range (8 to 12 Hz) (Fig. 2C). This provided a continuous estimate of alpha oscillatory power (not total alpha power) for each time point in each trial (Fig. 2D, dark purple line). These sliding-window estimates of the aperiodic exponent and alpha oscillatory power were then used with the alpha total power in subsequent analyses.

To increase the signal-to-noise of these sliding-window estimates, the data were averaged across trials into three separate blocks. Trials were randomly assigned to one of the three blocks, but the same number of trials from each location bin were included in each block and the blocks were independent (i.e., no trial was included in multiple blocks). The values were then averaged across each block, such that the final matrix of parameter values was l location bins * b blocks \times m channels \times s time points.

Fitting Inverted Encoding Models. Similar to the procedure from the original papers (24, 25, 34), we fit inverted encoding models (IEMs) to reconstruct location-selective channel tuning functions (CTFs) from the topographic

distribution of each parameter (alpha and aperiodic) across electrodes. This was done separately for alpha total power values from the Hilbert transform and the aperiodic exponent and alpha oscillatory power values from spectral parameterization. We assumed that the parameter value at each electrode reflects the weighted sum of eight spatially tuned channels (i.e., neuronal populations), each tuned for a different angular location (24, 37). Each spatial channel's response across angular locations was modeled as a half sinusoid raised to the seventh power, given by

$$R = \sin(0.5\theta)^7,$$
 [1]

where θ is angular location (ranging from 0° to 359°), and R is the response of the spatial channel in arbitrary units. This response profile was circularly shifted for each channel such that the peak response of each spatial channel was centered over one of the eight location bins (i.e., 0°, 45°, 90°, etc.). The predicted channel responses for each location bin were derived from these basis functions (calculated using the angular location at the center of each bin).

First, encoding models were fit separately to the alpha total power, aperiodic exponent, and alpha oscillatory power values for each time point (Fig. 3 A–D). Data from the first two blocks were used for training, while the third was held-out for testing (described below). Let ${\bf B_{train}}$ (m electrodes \times n_{train} observations) be the parameter value at each electrode for each measurement in the training set (Fig. 3C), with ${\bf C_{train}}$ (k channels \times n_{train} observations) being the predicted response of each spatial channel (determined by the basis functions) for each measurement (Fig. 3B), and ${\bf W}$ (m electrodes \times k channels) being a weight matrix that characterizes a linear mapping from "channel space" to "electrode space." The relationship between ${\bf B_{train}}$, ${\bf C_{train}}$, and ${\bf W}$ can be described by a general linear model of the form:

$$B_{train} = WC_{train}.$$
 [2]

The weight matrix was fit to the training data using least-squares estimation:

$$W = B_{train} C_{train}^{T} (C_{train} C_{train}^{T})^{-1}.$$
 [3]

Second, the weights were then inverted and used to transform the test data $\mathbf{B_{test}}$ (m electrodes \times n_{test} observations) into estimated channel response $\mathbf{C_{test}}$ (k channels \times n_{train} observations, Fig. 3F):

$$\mathbf{C}_{\text{test}} = (\mathbf{W}^{\mathsf{T}} \mathbf{W})^{-1} \mathbf{W}^{\mathsf{T}} \mathbf{B}_{\text{test}}.$$
 [4]

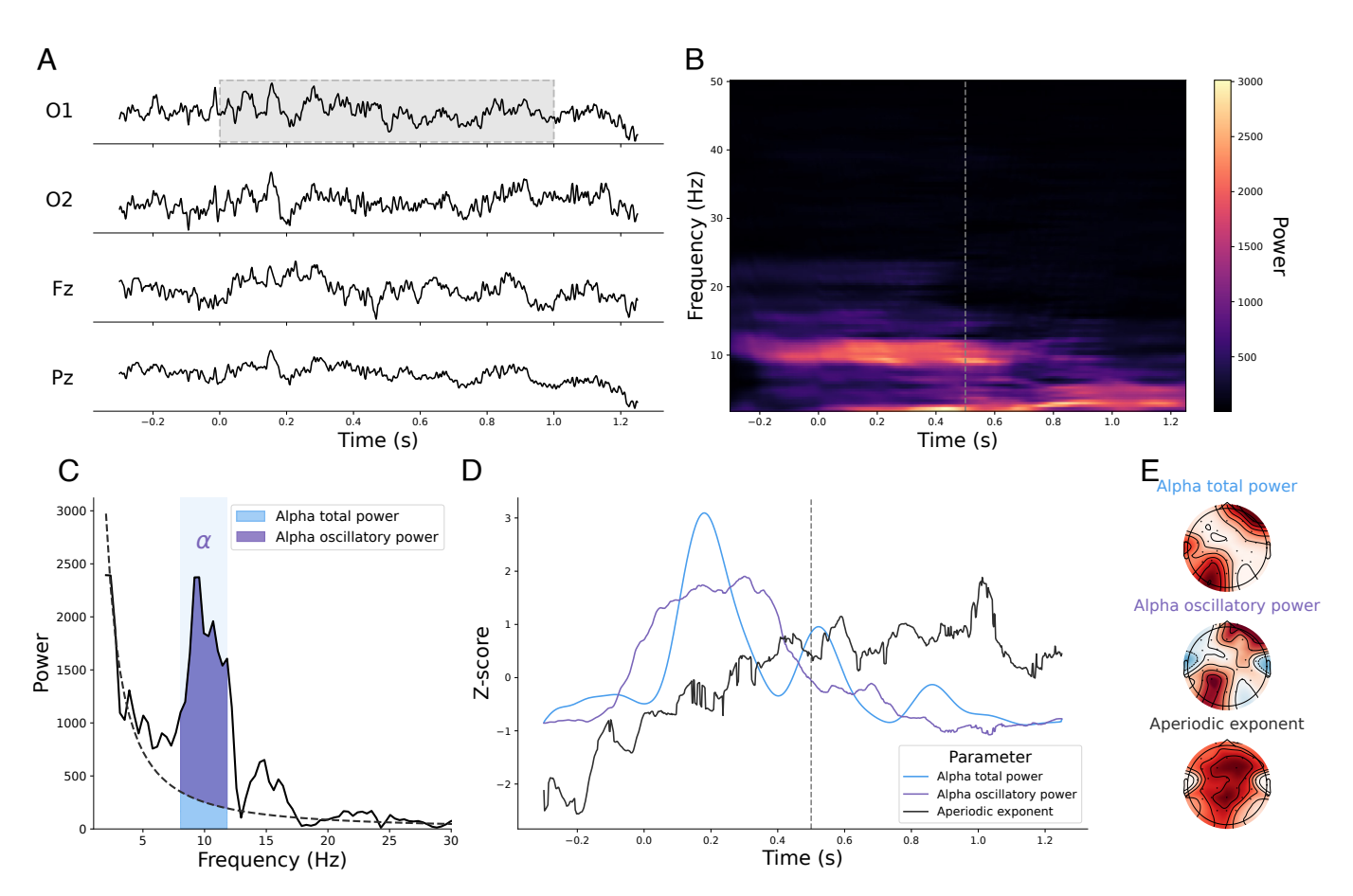


Fig. 2. Estimation of time-resolved aperiodic and aperiodic-adjusted oscillatory parameters for individual trials. (A) Voltage traces from one trial for two occipital channels (O1, O2), one parietal channel (Pz), and one frontal channel (Fz). The gray bounding box highlights the one-second temporal window that serves as input for multitaper decomposition to estimate the spectral properties for the time point 0.5 s after stimulus presentation. (B) Multitaper spectrogram for one occipital channel (O1) for the same trial as shown in (A). The vertical gray dashed line denotes the time point 0.5 s after stimulus presentation. (C) Power spectrum for the time window and channel denoted in (B), which is used to estimate the "instantaneous" spectral parameters. Alpha total power (hashed window) is the full area under the curve (AUC) within the alpha band (8 to 12 Hz, light purple), while alpha oscillatory power is the alpha total power minus the power attributed to the aperiodic exponent (dark purple). (D) Time-resolved estimates of alpha total power, alpha oscillatory power, and the aperiodic exponent for the same trial as shown in (A) for channel O1. (E) Spatial distribution of alpha total power, alpha oscillatory power, and aperiodic exponent for same time point and trial shown in (A).

Each estimated channel response function was circularly shifted to a common center by aligning the estimated channel responses to the channel tuned for the stimulus bin to yield CTFs (Fig. 3H). This procedure of fitting an encoding model on the training data **B**_{train} and inverting that encoding model to estimate the channel responses for the test data **B**_{test} was repeated for each time point and with each block serving as the test block, such that we performed a "leave-one-out" cross-validation. The resulting CTFs were averaged across the three testing blocks. Finally, the procedure was repeated for 100 block assignments for each participant to minimize the influence of idiosyncrasies in estimates of parameter values specific to certain assignments of trials to blocks.

Statistical Analyses. CTFs were circularly shifted to the correct spatial location and reflected about that spatial location, such that points equidistant from the correct spatial location are treated identically. To estimate the representation strength of the correct spatial location, the slope of the linear regression for these transformed CTFs was calculated, hereafter referred to as the CTF slope (Fig. 31). We z-scored the CTF slopes for each participant based on the baseline period, such that CTF slope values above 1.96 indicate P < 0.05. We computed one-sample t tests to evaluate whether CTF slopes in the encoding and delay periods differed significantly from the baseline (which would have a z-scored CTF slope of 0 by design). Comparisons between parameters (e.g., alpha total power and alpha oscillatory power) were made using paired t tests across participants. We accounted for multiple comparisons using the Benjamini-Hochberg procedure (38).

Results

Time Courses of Spatial Location Representation Are Consistent Across Seven Different Working Memory Tasks. We reconstructed the time courses of spatial location representation by alpha total power, alpha oscillatory power, and the aperiodic exponent for each of the seven WM tasks in the composite dataset (Fig. 4). Time courses of spatial location representation by the aperiodic offset are very similar to those of the aperiodic exponent (SI Appendix, Fig. S1), which is expected given their strong correlation (SI Appendix, Fig. S2, blue). Importantly, these tasks had different stimulus durations, task-relevant features, and were collected across two different sites. Yet, the time courses of spatial location representation by these features were consistent across tasks, with the spatial location representation by alpha total power and alpha oscillatory power peaking during the delay period and the spatial location representation by aperiodic activity peaking during the encoding period. Alpha total power, alpha oscillatory power, and the aperiodic exponent are all very weakly correlated throughout the trial across all tasks (SI Appendix, Fig. S2), bolstering the notion that these are largely independent processes.

Alpha Power Represents the Correct Spatial Location During the Delay Period. We performed one-sample t tests on the z-scored CTF slopes across participants for each task. The

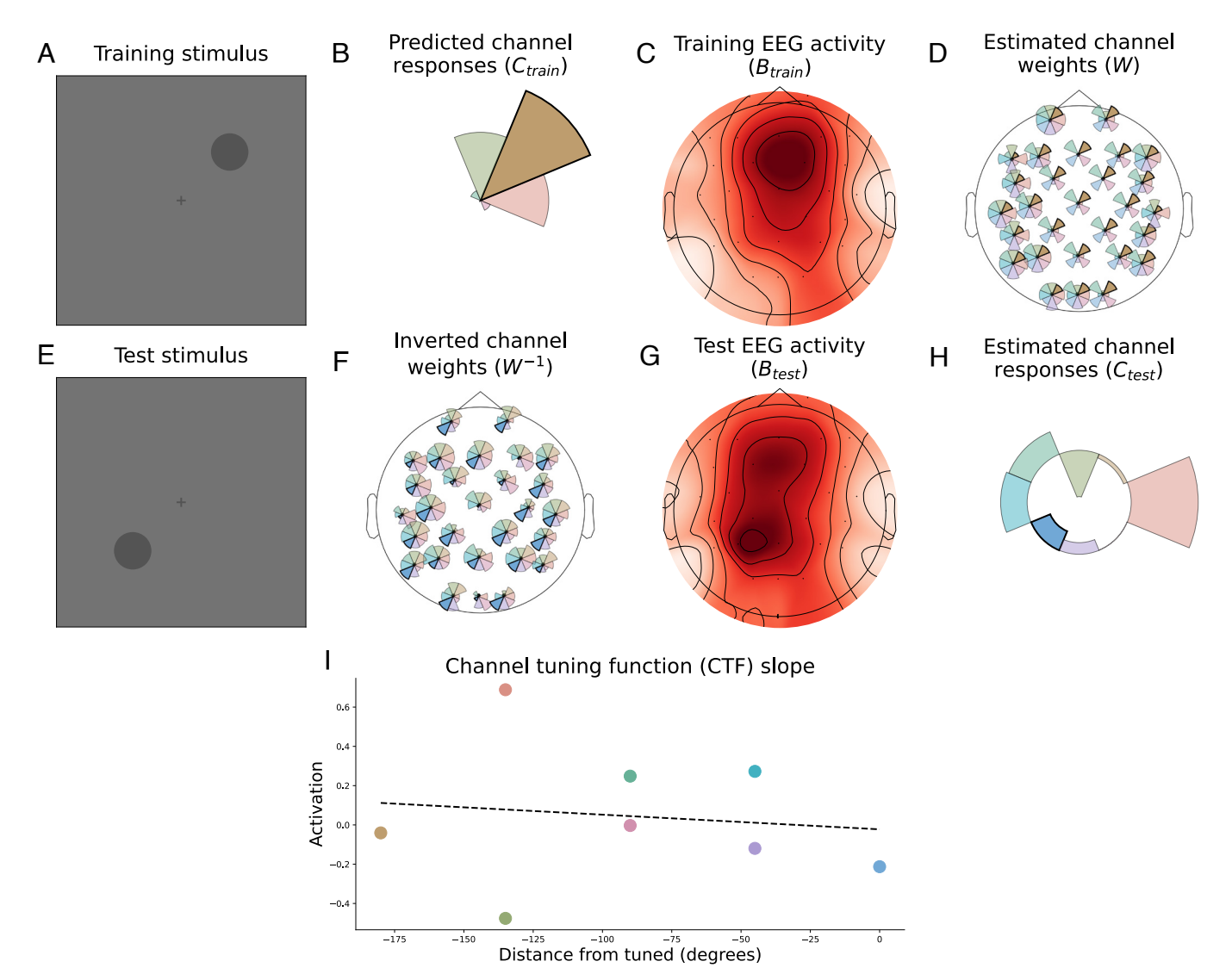


Fig. 3. Procedure for fitting inverted encoding models to estimate strength of representation for correct spatial location. (*A*) Training stimulus presented at 45°. (*B*) Predicted spatial channel response for neural populations encoding each of the eight location bins for the stimulus presented at 45°. The spatial channel response is modeled using Eq. **1**. This corresponds to one row of **C**_{train}. (*C*) Average EEG activity for each sensor for one example training block. The topomap shown is the average, aperiodic-adjusted alpha oscillatory power at 0.5 s for each sensor for one participant. Each row in **B**_{train} represents alpha oscillatory power at 0.5 s across each sensor for each trial. (*D*) The estimated channel weights fit from the predicted channel responses and alpha oscillatory power using Eq. **3**. The weights corresponding to the training stimulus shown at 45° are highlighted for each sensor. (*E*) Test stimulus presented at 225°. (*F*) Inverted channel weights as shown in Eq. **4**. The weights corresponding to the test stimulus shown at 225° are highlighted for each sensor. (*G*) Average EEG activity for each sensor for one example test block. The topomap shown is the average alpha oscillatory power at 0.5 s for each sensor for one participant. Each row in **B**_{test} represents alpha oscillatory power at 0.5 s across each sensor for each trial. (*H*) Estimated spatial channel response for neural populations encoding each of the eight location bins for a stimulus presented at 225°, as calculated by Eq. **4**. (*I*) Channel tuning function (CTF) slope, calculated after the spatial estimated channel response shown in (*H*) is circularly shifted to the correct spatial location and reflected about that spatial location. The dotted line shows the slope of the linear regression of this CTF for stimuli presented at 225° for this test block.

representation of the correct spatial location during the delay period by alpha total power and by alpha oscillatory was significant across all seven tasks (Fig. 5 A and B, respectively). The representation of the correct spatial location during the encoding period by alpha total power was also significant for four of the seven tasks, while that by alpha oscillatory power was significant for five of the seven tasks.

To determine whether the strength of representation was significantly different between the encoding and delay periods, we also performed paired t tests between the z-scored CTF slopes during the encoding and delay periods. Alpha total power represented the correct spatial location significantly more strongly during the delay, compared to the encoding period, in four of seven tasks, while the encoding period representation was stronger compared to the delay in one task (Fig. 5A).

Alpha oscillatory power represented the correct spatial location significantly more strongly during the delay, compared to the encoding period, in four tasks; in the other three tasks, the difference between the encoding and delay period was not significant (Fig. 5*B*).

Aperiodic Exponent Represents the Correct Spatial Location During the Encoding Period. The representation of the correct spatial location during the encoding period by aperiodic exponent was significant across all seven tasks (Fig. 5C). The aperiodic exponent showed significant representation of the correct spatial location during the delay period in five of the seven tasks. Finally, the representation of the correct spatial location by the aperiodic exponent was significantly stronger during the encoding, compared to the delay period, in six of the seven tasks.

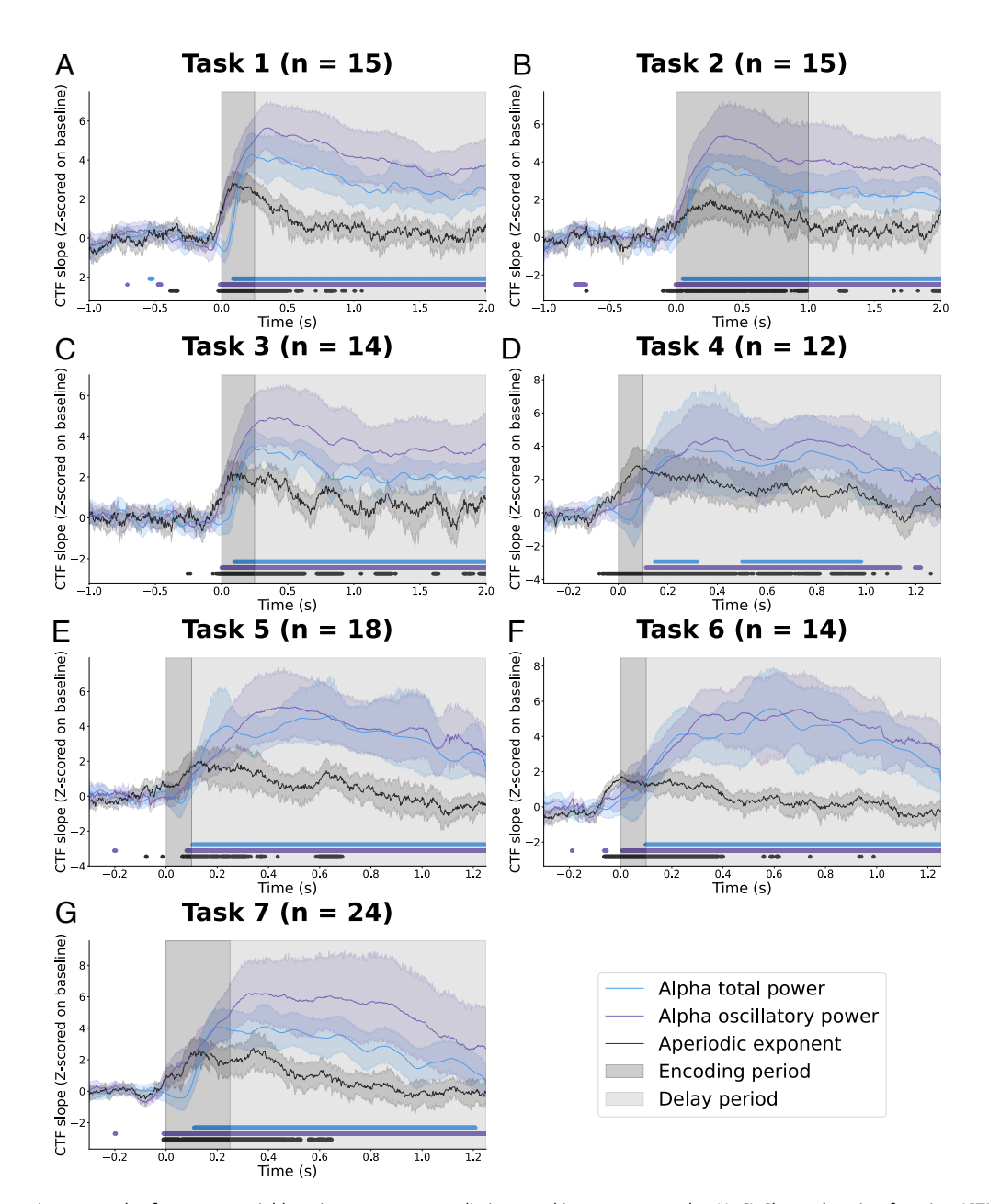


Fig. 4. Representation strength of correct spatial location across seven distinct working memory tasks. (*A*–*G*) Channel tuning function (CTF) slope, *z*-scored on the baseline period, across each of the seven WM tasks for spatial location by alpha total power (blue), alpha oscillatory power (purple), and the aperiodic exponent (black). The shading of lines reflects the 95% CIs across participants within each task. The dots at the *Bottom* of the plot indicate when one-sample, one-tailed *t* tests against zero are significant following FDR correction. The darker vertical shading designates the encoding period, while the lighter shading designates the delay period.

Alpha Oscillatory Power Better Represents the Correct Spatial Location During the Delay Period than Alpha Total Power.

Alpha oscillatory power represented the correct spatial location better than alpha total power during the delay in 85 out of 112 participants (Fig. 5D). To test whether the representation of the correct spatial location by alpha oscillatory power was significantly stronger than that by alpha total power, we computed paired t tests between each participant's alpha oscillatory power and alpha total power CTF slopes within each task, correcting for multiple comparisons across tasks. The representation of the correct spatial location was significantly stronger in six of the seven tasks (Fig. 5D, legend), suggesting that alpha oscillatory power better captures spatial location information than alpha total power.

Discussion

In this paper, we applied time-resolved spectral parameterization to estimate continuous aperiodic-adjusted alpha power (i.e., alpha oscillatory power) and aperiodic activity across a composite dataset comprising 112 participants and seven different WM tasks. We first replicated previous findings of significant representation of the correct spatial location by alpha total power during the delay period. After adjusting for contributions of aperiodic activity to these alpha power estimates, we showed significant improvements in the strength of spatial location representation. Finally, we uncovered a role for aperiodic activity within the context of working memory-the aperiodic exponent encodes spatial location during stimulus presentation. Together,

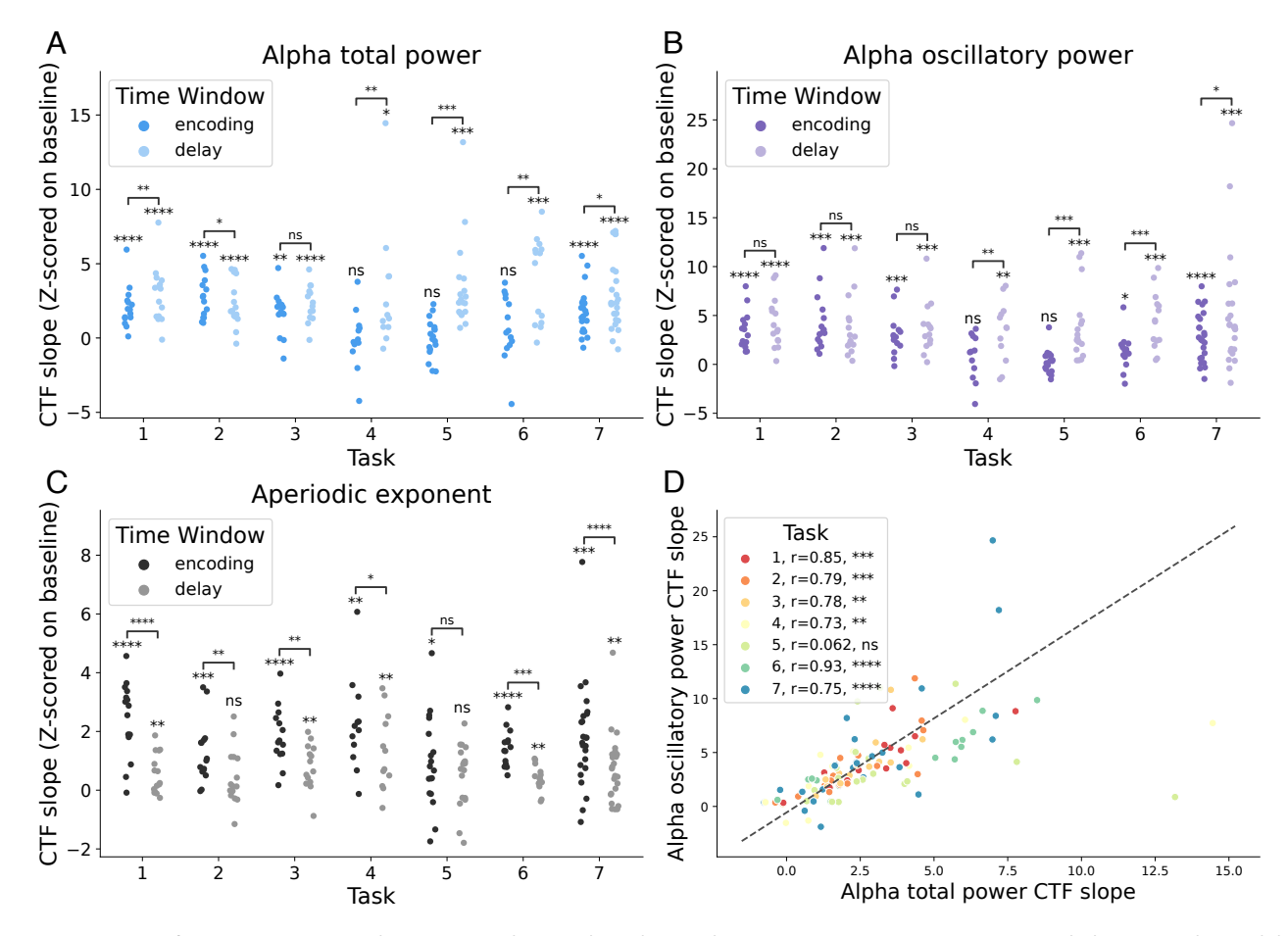


Fig. 5. Comparison of representation strength time courses by periodic and aperiodic parameters. (*A*) Representation strength during encoding and delay periods for each participant by alpha total power, (*B*) alpha oscillatory power, and (*C*) aperiodic exponent. Significance above each cluster reflects the deviation from baseline for each time period, while the significance between clusters reflects the paired difference between the encoding and delay time periods across participants. (*D*) Comparison of representation strength by alpha oscillatory power and alpha total power during the delay period for each participant. Values above the diagonal indicate stronger representation of the correct spatial location by alpha oscillatory power than alpha total power. The significance of the paired *t* test for each participant's representation strength of the correct spatial location by alpha oscillatory power versus that by alpha total power across each task is shown in the legend.

these results suggest alpha oscillations and aperiodic activity play distinct roles in the encoding and retention of spatial location during working memory.

Implications. The fact that alpha oscillatory power represents the correct spatial location significantly more strongly than alpha total power in six of the seven tasks shows that traditional analysis approaches that conflate oscillations with aperiodic activity are impairing our ability to understand the functional role of neural oscillations while also hiding the potentially distinct functional role of aperiodic activity. Our results show that alpha oscillatory power more closely reflects the processes involved in the retention of spatial location in visual WM. These results highlight the importance of removing aperiodic contributions to measures of oscillatory activity, even if aperiodic activity is not the focus of investigation. Apart from its role in WM, differences in alpha total power have been observed in the context of many cognitive functions and cognitive disorders (39-42). In these studies, researchers most commonly use measures of alpha power that do not account for aperiodic activity. Our results across these seven WM tasks demonstrate that using an aperiodic-adjusted measure of alpha power may provide a more sensitive measure of alpha oscillatory activity. Moreover, there may be interesting differences in aperiodic activity that coincide with those already observed in alpha total power.

Aperiodic activity has been shown to capture information about its underlying physiological generators, such as the relative balance of excitation and inhibition (27). Moreover, small, dynamic fluctuations in excitation-inhibition balance are critical for healthy cognitive functioning, allowing for efficient information transmission and gating (43), network computation (44), top-down attentional gain modulation (45-47), and WM maintenance(48). The model of aperiodic activity developed by Gao and colleagues (27) suggests that an increase in excitation necessary for encoding the stimulus would manifest as a decrease in the aperiodic exponent, leading to a flattening of the power spectrum. Recent work has shown a flattening of the power spectrum in intracranial EEG during memory encoding that is consistent with this hypothesis (49). Our result that the aperiodic exponent represents the correct spatial location during the encoding period is consistent with these previous findings and further validates the notion that the dynamic changes in the aperiodic exponent reflect increases in excitation necessary for stimulus encoding. Future studies are necessary to test directly whether an increase in excitation underlies the representation of spatial location by aperiodic exponent during encoding. Such studies would validate both the computational model of aperiodic activity as reflective of relative balance in excitation and inhibition and the role of excitation-inhibition interactions in encoding stimulus for WM.

Our results demonstrate that the aperiodic exponent represents spatial location during the encoding period, while alpha oscillatory activity represents spatial location during the delay period. Previous work has demonstrated that E-I interactions are essential for the formation of neural oscillations (50, 51), which suggests that oscillations and aperiodic activity interact.

Limitations. While alpha oscillatory activity more strongly represents spatial location than alpha total power in all but one of the seven WM tasks tested here, it is more computationally costly to do sliding-window spectral parameterization than to use traditional methods like a filter-Hilbert approach. That said, there are a couple of ways to reduce this computation time moving forward. First, the signal could be downsampled prior to applying sliding-window spectral parameterization. In this paper, we wanted to match the instantaneous alpha total power estimation from the filter-Hilbert approach as closely as possible to ensure a fair comparison. So, we performed no downsampling. Because there is substantial overlap in the windows used to compute spectral features from time point to time point, such time resolution is unnecessary. The computation time would be reduced by the decimation factor chosen, greatly reducing computation time. Future studies could also investigate combining independent sliding-window estimations of alpha total power (through a filter-Hilbert approach) and of the aperiodic exponent. Importantly, while both the filter-Hilbert and sliding-window spectral parameterization approaches yield amplitude estimates at each sample, their effective temporal resolution is constrained-by the filter bandwidth in the former and the window length in the latter. Here, we used an 8 to 12 Hz bandpass filter and 1-s sliding windows, corresponding to effective temporal resolutions of approximately 250 ms and ± 500 ms, respectively. Tuning these hyperparameters to optimize temporal or spectral resolution may be beneficial in future work.

In addition to the computational costs, there are fundamental questions surrounding how to identify oscillations. Although we took a spectral parameterization approach, there are several emerging methods for separating oscillations from aperiodic activity in both the time (52, 53) and frequency domains (54). Furthermore, there are more fundamental questions about how sensitive our methods are for even identifying oscillations in the first place (55), though there are methods for enhancing the oscillation signal-to-noise (56, 57). Finally, this analysis was constrained to looking at alpha power, though there are likely significant effects of alpha phase in working memory (21, 58, 59), and potentially even with regard to the subtle differences in the alpha waveform (60, 61).

In terms of the kinds of tasks analyzed, this composite dataset worked well to investigate whether adjusting for aperiodic activity in estimating instantaneous alpha power substantially improved reconstruction of spatial location information in WM across an expansive number of WM tasks and participants. This investigation revealed an interesting contribution of aperiodic activity in representing spatial location during encoding, but the tasks were not designed to explicitly test for aperiodic activity and its role in encoding. Various modifications to the experimental task would allow for a more thorough examination of aperiodic activity's role in WM encoding. First, using multiple stimuli and a precue that identifies which stimulus is the target (i.e., should then be attended to) and which stimulus is the distractor (i.e., should not be attended to) would allow researchers to disambiguate whether aperiodic activity tracks attention-agnostic, stimulus-driven activity, or attentive perception. Second, stimulus presentation was 250 ms or less in six of the seven tasks we analyzed; longer

encoding periods would improve time-frequency analyses and ensure more of the time-frequency decomposition is computed with windows that are exclusively from the encoding period. Recent work by Tsubomi and colleagues demonstrated WM content is spontaneously removed after it becomes obsolete, suggesting WM is goal-directed and sensitive to task timing (62). Manipulation of the length of the encoding period would allow for a similar test of sensitivity to task timing for the aperiodic exponent. Third, a WM task with serial presentation (e.g., Sternberg task) would allow researchers to evaluate whether each memory item is successively encoded by aperiodic activity since the corresponding neural activity will be separated in time. This would complement previous work that has suggested that sequential and simultaneous presentations rely on similar WM processes. For example, Woodman and colleagues showed that sequential and simultaneous presentation resulted in similar WM accuracy across different set sizes (63), while Zhao and Vogel showed that performance is highly correlated in sequential and simultaneous WM tasks across individuals (64). Finally, similar to work done by Waschke and colleagues (30), researchers could experimentally manipulate the stimuli to bias aperiodic activity in the visual cortex and examine how such biasing affects WM encoding. Such an experiment would also enable explicit testing of the interaction between stimulus encoding by aperiodic activity and WM maintenance by alpha oscillatory activity.

Conclusion. These results support the idea that alpha oscillations are associated with the maintenance of spatial location information in WM, highlighting that it really is the oscillations' power that is most relevant, not the total power. We developed spectral methods for sliding-window estimation of alpha oscillatory power and aperiodic activity. These time-resolved methods enabled us to disambiguate distinct roles for alpha oscillations and aperiodic activity in WM that had previously been mixed in the alpha total power signal. Specifically, aperiodic activity encodes spatial location during stimulus presentation, while the power of alpha oscillations maintain spatial location information throughout the WM delay. By leveraging sliding-window spectral parameterization, new experiments designed to test explicitly for the role of aperiodic activity in encoding could provide further mechanistic insights into how these distinct neural components contribute to WM encoding and maintenance. While the poor spatial resolution of scalp EEG may be masking differences in cortical processing of aperiodic and oscillatory activity, one implication of our results is that incoming visual sensory information drives cortical excitation in a topographic manner, but that this asynchronous, aperiodic drive is then translated into an oscillatory code for maintenance. Whether such an interaction between oscillations and periodic activity underlie encoding and maintenance of information in visual WM remains an open question.

Data, Materials, and Software Availability. Previously published data were used for this work (24, 25, 34).

ACKNOWLEDGMENTS. We thank Thomas Donoghue, Ryan Hammonds, Michael Preston, Natalie Schaworonkow, and John Serences for their thoughtful advice and feedback on the manuscript.

Author affiliations: ^aNeurosciences Graduate Program, University of California, San Diego, La Jolla, CA 92093; ^bDepartment of Psychology, The University of Chicago, Chicago, IL 60637; ^cInstitute for Mind and Biology, Division of Social Sciences, The University of Chicago, Chicago, IL 60637; ^dDepartment of Cognitive Science, University of California, San Diego, La Jolla, CA 92093; ^eHalicioğlu Data Science Institute, University of California, San Diego, La Jolla, CA 92093; and ^f Kavli Institute for Brain and Mind, University of California, San Diego, La Jolla, CA 92093

- T. B. Christophel, P. C. Klink, B. Spitzer, P. R. Roelfsema, J. D. Haynes, The distributed nature of working memory. Trends Cogn. Sci. 21, 111-124 (2017).
- M. Stokes et al., Dynamic coding for cognitive control in prefrontal cortex. Neuron 78, 364-375
- T. B. Christophel, M. N. Hebart, J. D. Haynes, Decoding the contents of visual short-term memory from human visual and parietal cortex. J. Neurosci. 32, 12983-12989 (2012).
- S. A. Harrison, F. Tong, Decoding reveals the contents of visual working memory in early visual areas. Nature 458, 632-635 (2009).
- A. C. Riggall, B. R. Postle, The relationship between working memory storage and elevated activity as measured with functional magnetic resonance imaging. J. Neurosci. 32, 12990-12998
- J. T. Sérences, E. F. Ester, E. K. Vogel, E. Awh, Stimulus-specific delay activity in human primary visual cortex. *Psychol. Sci.* **20**, 207–214 (2009).
- K. K. Sreenivasan, J. Vytlacil, M. D'Esposito, Distributed and dynamic storage of working memory stimulus information in extrastriate cortex. J. Cogn. Neurosci. 26, 1141-1153 (2014).
- G. Buzsáki, C. A. Anastassiou, C. Koch, The origin of extracellular fields and currents EEG, ECoG, LFP and spikes. Nat. Rev. Neurosci. 13, 407-420 (2012).
- P. Fries, A mechanism for cognitive dynamics: Neuronal communication through neuronal coherence. Trends Cogn. Sci. 9, 474-480 (2005).
- O. Jensen, Oscillations in the alpha band (9-12 Hz) increase with memory load during retention in a short-term memory task. Cereb. Cortex 12, 877-882 (2002).
- D. Jokisch, O. Jensen, Modulation of gamma and alpha activity during a working memory task engaging the dorsal or ventral stream. J. Neurosci. 27, 3244-3251 (2007).
- W. Klimesch, Alpha-band oscillations, attention, and controlled access to stored information. Trends Cogn. Sci. 16, 606-617 (2012).
- 13. F. van Ede, O. Jensen, E. Maris, Supramodal theta, gamma, and sustained fields predict modalityspecific modulations of alpha and beta oscillations during visual and tactile working memory. J. Cogn. Neurosci. **29**, 1455–1472 (2017).
- 14. K. C. S. Adam, M. K. Robison, E. K. Vogel, Contralateral delay activity tracks fluctuations in working
- N. C. S. Rudni, M. R. Nobisoni, E. R. Wege, Contralateral delay activity tacks includations in working memory performance. J. Cogn. Neurosci. 30, 1229–1240 (2018).
 Q. van Engen et al., Dissociating contributions of theta and alpha oscillations from aperiodic neural activity in human visual working memory. bioRxiv [Preprint] (2024). https://www.biorxiv.org/content/10.1101/2024.12.16.628786v1.full (Accessed 20 March 2025).
- 16. B. Spitzer, F. Blankenburg, Supramodal parametric working memory processing in humans. J. Neurosci. 32, 3287-3295 (2012).
- 17. F. van Ede, Mnemonic and attentional roles for states of attenuated alpha oscillations in perceptual working memory: A review. Eur. J. Neurosci. 48, 2509-2515 (2018).
- 18. W. P. Medendorp et al., Oscillatory activity in human parietal and occipital cortex shows hemispheric lateralization and memory effects in a delayed double-step saccade task. Cereb. Cortex 17, 2364-2374 (2007).
- 19. J. Van Der Werf, O. Jensen, P. Fries, W. P. Medendorp, Gamma-band activity in human posterior parietal cortex encodes the motor goal during delayed prosaccades and antisaccades. J. Neurosci.
- 20. H. van Dijk, J. van der Werf, A. Mazaheri, W. P. Medendorp, O. Jensen, Modulations in oscillatory activity with amplitude asymmetry can produce cognitively relevant event-related responses. Proc. Natl. Acad. Sci. U.S.A. 107, 900-905 (2010).
- T. T. Tran, N. C. Hoffner, S. C. LaHue, L. Tseng, B. Voytek, Alpha phase dynamics predict age-related visual working memory decline. *NeuroImage* 143, 196–203 (2016).
- 22. B. Voytek, R. T. Knight, Prefrontal cortex and basal ganglia contributions to visual working memory. Proc. Natl. Acad. Sci. U.S.A. 107, 18167–18172 (2010).
- 23. G. Y. Bae, S. J. Luck, Dissociable decoding of spatial attention and working memory from EEG oscillations and sustained potentials. J. Neurosci. 38, 409-422 (2018).
- J. J. Foster, D. W. Sutterer, J. T. Serences, E. K. Vogel, E. Awh, The topography of alpha-band activity tracks the content of spatial working memory. J. Neurophysiol. 115, 168-177 (2016).
- 25. J. J. Foster, E. M. Bsales, R. J. Jaffe, E. Awh, Alpha-band activity reveals spontaneous representations of spatial position in visual working memory. Curr. Biol. 27, 3216-3223.e6 (2017).
- 26. M. Chini, T. Pfeffer, I. Hanganu-Opatz, An increase of inhibition drives the developmental decorrelation of neural activity. eLife 11, e78811 (2022).
- R. Gao, E. J. Peterson, B. Voytek, Inferring synaptic excitation/inhibition balance from field potentials. NeuroImage 158, 70-78 (2017).
- 28. T. T. Tran, C. E. Rolle, A. Gazzaley, B. Voytek, Linked sources of neural noise contribute to age-related cognitive decline. J. Cogn. Neurosci. 32, 1813-1822 (2020).
- 29. B. Voytek et al., Age-related changes in 1/f neural electrophysiological noise. J. Neurosci. 35, 13257-13265 (2015).
- L. Waschke, M. Wöstmann, J. Obleser, States and traits of neural irregularity in the age-varying human brain. Sci. Rep. 7, 17381 (2017).
- 31. A. B. Arnett, V. Peisch, A. R. Levin, The role of aperiodic spectral slope in event-related potentials and cognition among children with and without attention deficit hyperactivity disorder. J. Neurophysiol. 128, 1546-1554 (2022).

- 32. T. Donoghue et al., Parameterizing neural power spectra into periodic and aperiodic components. Nat. Neurosci. 23, 1655-1665 (2020).
- 33. T. Donoghue, N. Schaworonkow, B. Voytek, Methodological considerations for studying neural oscillations. Eur. J. Neurosci. 55, 3502-3527 (2021).
- 34. D. W. Sutterer, J. J. Foster, K. C. S. Adam, E. K. Vogel, E. Awh, Item-specific delay activity demonstrates concurrent storage of multiple active neural representations in working memory. PLoS Biol. 17, e3000239 (2019).
- 35. A. Gramfort, MEG and EEG data analysis with MNE-Python. Front. Neurosci. 7, 267 (2013).
- 36. A. Bruns, Fourier-, Hilbert- and wavelet-based signal analysis: are they really different approaches? J. Neurosci. Methods 137, 321-332 (2004).
- 37. T. Sprague, E. Ester, J. Serences, Reconstructions of information in visual spatial working memory
- degrade with memory load. *Curr. Biol.* **24**, 2174–2180 (2014).

 38. Y. Benjamini, Y. Hochberg, Controlling the false discovery rate: A practical and powerful approach to multiple testing. *J. R. Stat. Soc. Ser. B Stat. Methodol.* **57**, 289–300 (1995).
- E. Başar, M. Schürmann, C. Başar-Eroglu, S. Karakaş, Alpha oscillations in brain functioning: An integrative theory. Int. J. Psychophysiol. 26, 5-29 (1997).
- W. Klimesch, P. Sauseng, S. Hanslmayr, EEG alpha oscillations: The inhibition-timing hypothesis. Brain Res. Rev. 53, 63-88 (2007).
- 41. S. Palva, J. M. Palva, New vistas for α -frequency band oscillations. *Trends Neurosci.* **30**, 150–158 (2007)
- 42. P. J. Uhlhaas, C. Haenschel, D. Nikolic, W. Singer, The role of oscillations and synchrony in cortical networks and their putative relevance for the pathophysiology of schizophrenia. Schizophr. Bull. 34, 927-943 (2008).
- 43. T. P. Vogels, L. F. Abbott, Gating multiple signals through detailed balance of excitation and inhibition in spiking networks. Nat. Neurosci. 12, 483-491 (2009).
- J. Mariño et al., Invariant computations in local cortical networks with balanced excitation and inhibition. Nat. Neurosci. 8, 194-201 (2005).
- 45. F. S. Chance, L. Abbott, A. D. Reyes, Gain modulation from background synaptic input. Neuron 35, 773-782 (2002).
- 46. D. A. Kaliukhovich, R. Vogels, Divisive normalization predicts adaptation-induced response changes in macaque inferior temporal cortex. *J. Neurosci.* **36**, 6116-6128 (2016).

 47. J. H. Reynolds, D. J. Heeger, The normalization model of attention. *Neuro* **61**, 168–185 (2009).

 48. S. Lim, M. S. Goldman, Balanced cortical microcircuitry for maintaining information in working
- memory. Nat. Neurosci. 16, 1306-1314 (2013).
- M. Preston, N. Schaworonkow, B. Voytek, Time-resolved aperiodic and oscillatory dynamics during human visual memory encoding. J. Neurosci. 45, e2404242025 (2025).
- 50. B. V. Atallah, M. Scanziani, Instantaneous modulation of gamma oscillation frequency by balancing excitation with inhibition. Neuron 62, 566-577 (2009).
- V. S. Sohal, F. Zhang, O. Yizhar, K. Deisseroth, Parvalbumin neurons and gamma rhythms enhance cortical circuit performance. Nature 459, 698-702 (2009).
- J. Q. Kosciessa, T. H. Grandy, D. D. Garrett, M. Werkle-Bergner, Single-trial characterization of neural rhythms: Potential and challenges. NeuroImage 206, 116331 (2020).
- R. A. Seymour, N. Alexander, E. A. Maguire, Robust estimation of 1/f activity improves oscillatory burst detection. Eur. J. Neurosci. 56, 5836-5852 (2022).
- 54. H. Wen, Z. Liu, Separating fractal and oscillatory components in the power spectrum of neurophysiological signal. Brain Topogr. 29, 13–26 (2016).
- S. van Bree, D. Levenstein, M. R. Krause, B. Voytek, R. Gao, Processes and measurements: a framework for understanding neural oscillations in field potentials. *Trends Cogn. Sci.* 29, \$1364661324003243 (2025).
- N. Schaworonkow, B. Voytek, Enhancing oscillations in intracranial electrophysiological recordings with data-driven spatial filters. *PLoS Comput. Biol.* 17, e1009298 (2021).
 N. Schaworonkow, V. V. Nikulin, Is sensor space analysis good enough? Spatial patterns as a tool for
- assessing spatial mixing of EEG/MEG rhythms NeuroImage 253, 119093 (2022).
- L. Ai, T. Ro, The phase of prestimulus alpha oscillations affects tactile perception. J. Neurophysiol. **111**, 1300-1307 (2014).
- R. Freunberger, R. Fellinger, P. Sauseng, W. Gruber, W. Klimesch, Dissociation between phaselocked and nonphase-locked alpha oscillations in a working memory task. Hum. Brain Mapp. 30, 3417-3425 (2009).
- 60. A. Bender, B. Voytek, N. Schaworonkow, Resting-state alpha and mu rhythms change shape across development but lack diagnostic sensitivity for attention-deficit/hyperactivity disorder and autism. J. Cogn. Neurosci., in press.
- 61. S. Cole, B. Voytek, Brain oscillations and the importance of waveform shape. Trends Cogn. Sci. 21,
- H. Tsubomi, K. Fukuda, A. Kikumoto, U. Mayr, E. K. Vogel, Task termination triggers spontaneous removal of information from visual working memory. *Psychol. Sci.* 35, 995–1009 (2024).
 G. F. Woodman, E. K. Vogel, S. J. Luck, Flexibility in visual working memory: Accurate change
- detection in the face of irrelevant variations in position. Vis. Cogn. 20, 1-28 (2012).
- C. Zhao, E. K. Vogel, Sequential encoding paradigm reliably captures the individual differences from a simultaneous visual working memory task. Atten. Percept. Psychophysiol. 85, 366–376 (2023).